

Stability analysis and optimization of excavation method of double-arch tunnel with an extra-large span based on numerical investigation

Yiguo XUE*, Huimin GONG, Fanmeng KONG, Weimin YANG, Daohong QIU, Binghua ZHOU

Geotechnical and Structural Engineering Research Center, Shandong University, Jinan 250061, China

*Corresponding author: E-mail: xieagle@sdu.edu.cn

© Higher Education Press 2021

ABSTRACT The Xiamen Haicang double-arch tunnel has a maximum span of 45.73 m and a minimum burial depth of 5.8 m. A larger deformation or collapse of the tunnel is readily encountered during tunnel excavation. It is therefore necessary to select a construction approach that is suitable for double-arch tunnel projects with an extra-large span. In this study, three construction methods for double-arch tunnels with extra-large spans were numerically simulated. Subsequently, the deformation behavior and stress characteristics of the surrounding rock were obtained and compared. The results showed that the double-side-drift method with temporary vertical support achieves better adaptability in the construction of such tunnels, which can be observed from both the numerical results and *in situ* monitoring data. In addition, the improved temporary support plays a critical role in controlling the surrounding rock deformation. In addition, the disturbance resulting from the excavation of adjacent drifts was obvious, particularly the disturbance of the surrounding rock caused by the excavation of the middle drift. The present findings can serve as the initial guidelines for the construction of ultra-shallowly buried double-arch tunnels with extra-large spans.

KEYWORDS double-arch tunnel, triple-layer composite liner system, numerical modeling, stress analysis, settlement

1 Introduction

A double-arch tunnel is a particular form of tunnel engineering, and the two adjacent tunnels are connected by a middle partition wall. Double-arch tunnels possess advantages such as a small occupation area, high space utilization rate, and smooth route connection. Therefore, double-arch tunnels have been widely used in tunnel construction in recent years. However, double-arch tunnels are usually characterized by large excavation spans, shallow burial depths, various construction procedures, and complex support systems, which have negative impacts on the tunnel construction. Therefore, the design and construction of a double-arch tunnel are much more difficult than those of a single-arch tunnel [1,2].

In general, the tunnel face is divided into several temporary drifts using the subsection excavation method, which can improve the stability of the tunnel face and

effectively control the deformation of the surrounding rock [3]. Therefore, during the construction of a large-span single-arch tunnel, subsection excavation methods, such as the center diaphragm method (CD), cross diaphragm method (CRD), and three-bench seven-step excavation method, are widely adopted. Academics and practitioners have conducted considerable research on subsection excavation methods for single-arch tunnels through field monitoring, physical model testing, numerical simulations, and engineering analogies [4–11]. However, few studies have been conducted on the construction methods of double-arch tunnels. Gao and Xue [12] compared and optimized three double-arch tunnel excavation procedures using the bench method. In addition, through a physical model test and numerical simulation, Li et al. [1] and Yang et al. [13] conducted an in-depth study on a CRD for the excavation of a double-arch tunnel. The corresponding regularity of the ground movement above the tunnel and the stress of shallowly buried formations were obtained. Furthermore, Bai et al. [14] and Yang et al. [15] carried out

a simulation analysis on the construction process of double-arch tunnel excavation using the three-tunnel method. Several scholars have also studied the structural stability and construction process optimization of double-arch tunnels under asymmetrical pressure and asymmetric double-arch tunnels [16,17].

Typical cases of double-arch tunnels with different spans were compared and analyzed (see Table 1). With an increase in the span, the excavation method and support system of the tunnel become increasingly complicated. The plastic zone of the surrounding rock displays a wider range of distribution in cases of double-arch tunnels with large spans. For example, the plastic zone above the middle partition wall of the Jinkou Tunnel (with a span of 22 m) has dimensions of 6.1 m \times 3.5 m, whereas the plastic zone above the middle partition wall of the Great Wall Ridge Tunnel (with a span of 33.97 m) has dimensions of 15 m \times 10 m. Furthermore, a wider tensile stress zone can also be seen at the arch crown and arch bottom of double-arch tunnels with large spans. The stress concentration phenomenon is more obvious at the arch foot and joint between the middle partition wall and the sidewall. Thus, the applicable construction approach is important for double-arch tunnels with an extra-large span. In previous construction cases of large-span tunnels, CD and CRD methods have usually been adopted (see Table 1). However, the use of a double-side-drift method in the excavation of an ultra-shallowly buried double-arch tunnel with an extra-large span has rarely been explored and studied. Meanwhile, the difference in the support performance of vertical or curved temporary support remains largely unexplained for the double-side-drift method.

After its completion, the double-arch tunnel of the Xiamen Haicang undersea tunnel will have the greatest across-span in China, as well as an ultra-shallow burial and complex geological engineering conditions. This study compared the deformation and stress characteristics of three construction methods, i.e., the CRD method, and the double-side-drift method with a vertical temporary support or a curved temporary support, in the excavation of a double-arch tunnel with an extra-large span. Based on both numerical results and *in situ* monitoring data, the best construction method and the optimized temporary support were developed for a double-arch tunnel. In addition, the displacement and stress field of the surrounding rock in each construction stage were analyzed for the double-side-

drift method with temporary vertical support. This study can provide a basis for optimizing the construction scheme, excavation sequence, and supporting parameters of a double-arch tunnel, which can then guide the field construction.

2 Project overview

The double-arch tunnel of the Xiamen Haicang undersea tunnel project has a total length of 160 m and is located in Huli District, Xiamen City, Fujian Province, China. The double-arch tunnel has a large excavation section, with a maximum double-line span of 45.73 m. The maximum burial depth of the double-arch tunnel is approximately 12.9 m, and the minimum burial depth of the double-arch tunnel is only 5.8 m [21].

The double-arch tunnel adopts the support form of a triple-layer composite liner system. The primary support is composed of a grouting steel pipe, H-shaped steel, steel mesh, and shotcrete. The secondary and temporary supports are composed of I-shaped steel, a steel mesh, and shotcrete, and the tertiary lining is composed of reinforced concrete. The tunnel adopts a compound middle wall 2–3.87 m thick (excluding the thickness of the tertiary lining).

Geotechnical engineering investigations have indicated that the geological engineering conditions of a tunnel construction are complex and that the rock exhibits clear variations in weathering. The strata above the double-arch tunnel are mainly composed of miscellaneous fill soil, highly weathered granite, and completely weathered granite. The rock surrounding the tunnel is mainly moderately weathered granite with poor integrity, and the surrounding rock at the bottom of the tunnel is mainly slightly weathered granite. The rock surrounding the double-arch tunnel has the characteristics of poor formation stability and rapid deformation.

3 Numerical simulation

3.1 Description of the numerical model

Three numerical simulation models, namely, a CRD method (Fig. 1(a)), a double-side-drift method with a

Table 1 Case information and statistics of typical double-arch tunnels

| tunnel name | span (m) | burial depth (m) | excavation methods of main tunnels | number of excavation sections | references |
|------------------|----------|------------------|------------------------------------|-------------------------------|-------------------|
| Jinkou | 22 | 45 | CD | 7 | Shen et al. [18] |
| Zhongxi | 25.19 | 38.52 | bench method | 5 | Zhang et al. [16] |
| Mazhaiding | 28.33 | 50 | CD | 9 | Wang et al. [19] |
| Zhangshi | 29.7 | 54 | bench method | 5 | Ji et al. [20] |
| Guanyinshan | 33.65 | 80 | CD | 12 | Yang et al. [15] |
| Great Wall ridge | 33.97 | 5 | CRD | 12 | Li et al. [1] |

temporary curved support (Fig. 1(b)), and a double-side-drift method with a vertical temporary support (Fig. 1(c)), were established. According to the disturbance range of the excavation and grid density, the length of the model is four-times the excavation span, and the distance from the bottom of the tunnel to the bottom part of the boundary is twice the height of the tunnel. As shown in Fig. 1, the numerical model is 52.97 m high, 174 m wide, and 20 m long. The strata in the model are miscellaneous fill soil, moderately weathered granite, and slightly weathered granite from top to bottom.

The top surface boundary of the calculation model was free. The horizontal constraint was set at the left and right sides of the model, the longitudinal constraint was set at the front and rear, and the vertical constraint was set to the bottom [22,23].

3.2 Constitutive model and calculated parameters

The Mohr–Coulomb model is a constitutive model that is widely used in geotechnical engineering and can be applied to simulate soil, rock, concrete, and loose cemented granular materials, among others. Therefore,

the Mohr–Coulomb model was adopted in this numerical simulation.

The calculated parameters of the surrounding rock were determined according to the design description of the Xiamen Haicang undersea tunnel. The elastic modulus of the steel arch and steel mesh are converted into shotcrete for an equivalent substitution. Furthermore, to simplify the calculation, the surrounding rock parameters of the reinforcement zone are improved to simulate the grouting area of the long pipe shed [12,24].

The calculation parameters of the surrounding rock used in the numerical simulation are listed in Table 2. The simulated parameters of the temporary support, primary support, secondary support, tertiary lining, and middle wall are shown in Table 3.

3.3 Excavation simulation

As shown in Fig. 2, the CRD method divides the tunnel section into nine drifts. The double-side-drift method with a vertical or curved temporary support divides the tunnel section into 13 drifts.

1) The CRD method consists of 15 specific construction

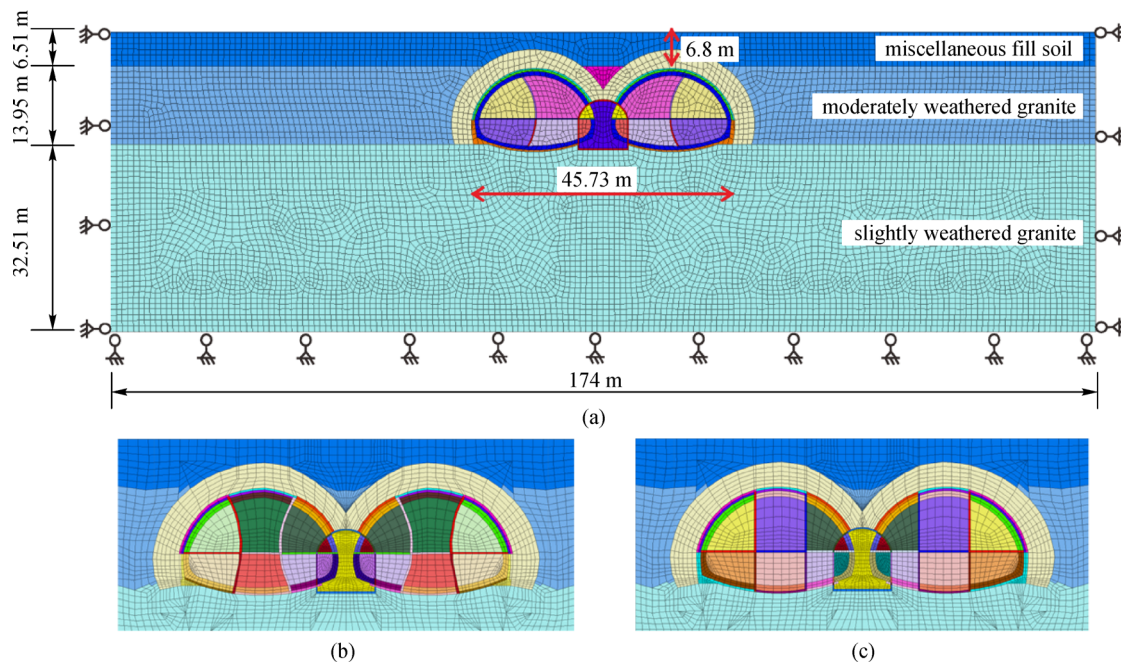


Fig. 1 The tunnel calculation model: (a) CRD method; (b) double-side-drift method with vertical temporary support; (c) double-side-drift method with curved temporary support.

Table 2 Physico-mechanical parameters of surrounding rock

| material name | unit weight (kN/m ³) | Poisson's ratio | Young's modulus (MPa) | cohesion (kPa) | friction angle (°) |
|------------------------------|----------------------------------|-----------------|-----------------------|----------------|--------------------|
| miscellaneous fill soil | 18.4 | 0.3 | 8.5 | 27 | 23 |
| moderately weathered granite | 25 | 0.25 | 6000 | 50 | 55 |
| slightly weathered granite | 26.5 | 0.2 | 15000 | 100 | 70 |

Table 3 Physico-mechanical parameters of the supporting structure

| material name | unit weight (kN/m ³) | Poisson's ratio | Young's modulus (MPa) |
|-------------------|----------------------------------|-----------------|-----------------------|
| temporary support | 22 | 0.2 | 25000 |
| primary support | 23 | 0.2 | 28000 |
| secondary support | 22 | 0.2 | 25000 |
| tertiary lining | 27 | 0.2 | 35000 |
| middle wall | 27 | 0.2 | 35000 |

stages.

Stages 1–3: Drifts No. 1 and 2 are excavated. The primary, temporary, and secondary supports are exerted after the excavation of each drift. The middle partition wall was poured after the excavation of middle drift No. 0. The arch foot of drift No. 2 overlaps with the middle partition wall during these phases.

Stages 4 and 5: Drifts No. 3 and 4 are excavated in turn, and primary, temporary, and secondary support are exerted. The arch foot of drift No. 3 overlaps with the middle partition wall during these phases.

Stages 6–9: Drifts No. 5 and 6 are excavated and supported. The tertiary lining of the left line is then applied after the removal of its temporary support.

Stages 10–13: Drifts No. 7 and 8 of the right line are successively excavated and supported. The tertiary lining of the right line is then applied after the removal of its temporary support.

2) The double-side-drift method with a vertical or curved temporary support consists of 17 specific construction stages.

Stages 1–3: Drifts No. 1 and 2 are excavated in turn after applying the long pipe shed above drifts No. 1 and 2. The primary, temporary, and secondary supports are exerted

after the excavation of each drift. The middle partition wall was then poured after the excavation of middle drift No. 0.

Stages 4–7: The primary supporting parts of middle drift No. 0 located in drifts No. 3 and 4 are removed after applying the long pipe shed above the drift. Then, drifts No. 3 and 4 are excavated in turn, and the primary, temporary, and secondary supports are exerted. The arch foot of drifts No. 3 and 4 overlaps with the middle partition wall in these phases. Then, drifts No. 5 and 6 are excavated and supported.

Stages 8–10: Drifts No. 7, 9, and 8 of the left line are successively excavated.

Stages 11–15: The tertiary lining of the left line is applied after the removal of its temporary support. Drifts No. 10, 12, and 11 of the right line are successively excavated and supported.

Stages 16 and 17: The tertiary lining of the right line is applied after the removal of its temporary support.

4 Numerical results

4.1 Stress analysis of surrounding rock

Figure 3 shows the vertical stress contours of the surrounding rock of the three construction methods after completion of the construction. In Fig. 3, negative values indicate compressive stress, and positive values indicate tensile stress. Figure 3 shows that the distribution of the stress field of the surrounding rock is basically symmetric after the excavation using the three construction methods. The maximum vertical stress of the surrounding rock, which is approximately 2.76 MPa, is located at the sidewalls on either side of the tunnel when using the CRD method. However, the vertical stress in the same area

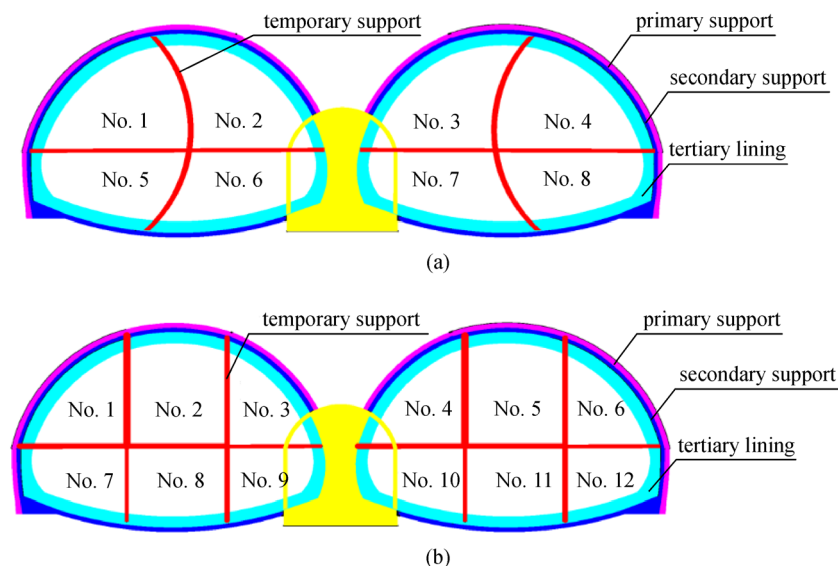


Fig. 2 Division of the tunnel section: (a) CRD method; (b) double-side-drift method.

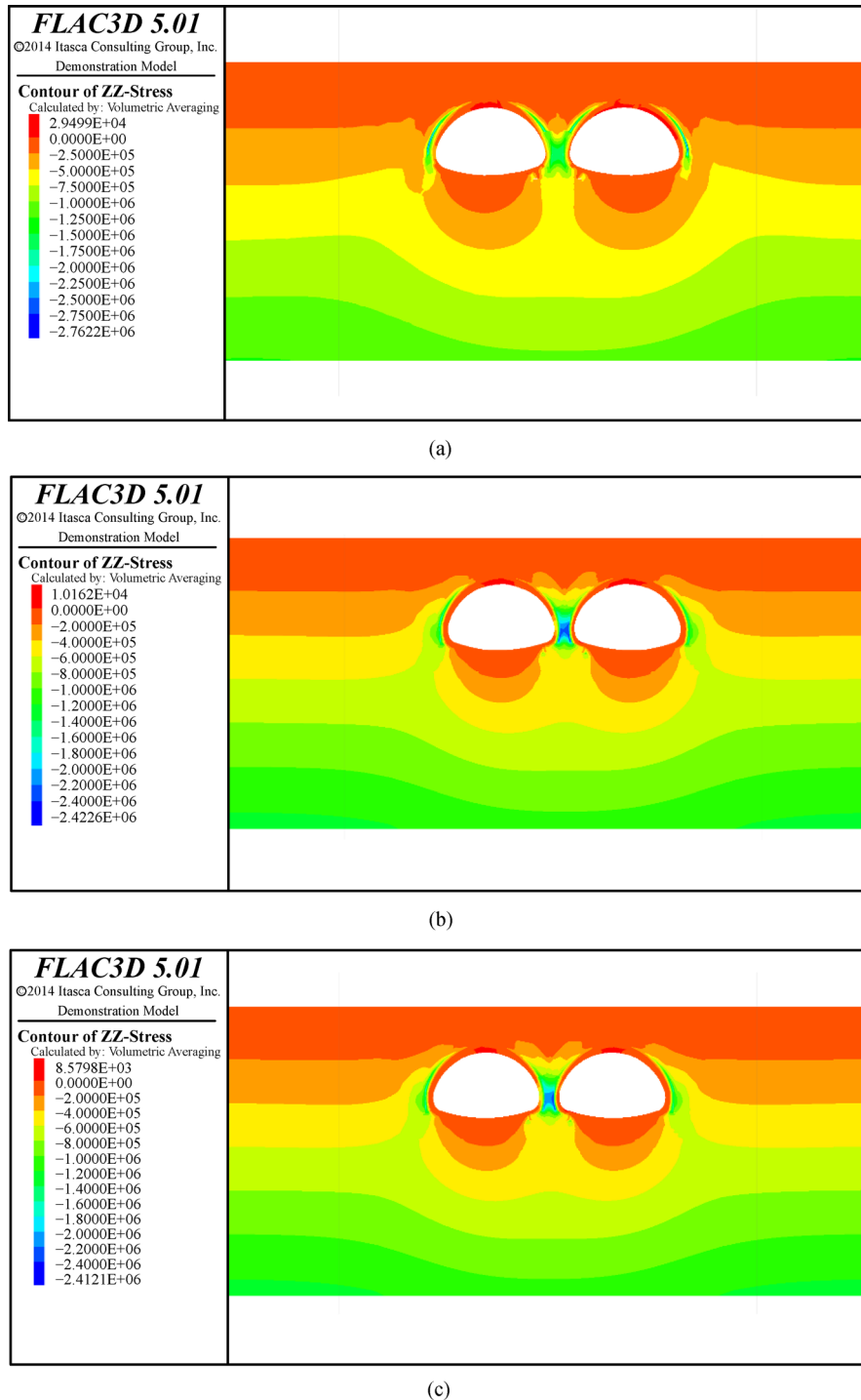


Fig. 3 Comparison of stress field of surrounding rock: (a) CRD method; (b) double-side-drift method with vertical temporary support; (c) double-side-drift method with curved temporary support (unit: Pa).

as that of the double-side-drift method is much less than that of the CRD method, at approximately 1.02 MPa. Meanwhile, when using the CRD method, spandrels close to the middle wall and the joint between the lining and middle wall exhibit a more obvious stress concentration. Furthermore, with the three construction methods, a tensile stress zone appears in the tunnel vault. The tensile stress

area is the largest when applying the CRD method and is the smallest when using the double-side-drift method with a temporary vertical support. Therefore, the double-side-drift method with a temporary vertical support is more beneficial to the stress redistribution of the surrounding rock during the construction of a double-arch tunnel with an extra-large span.

Owing to the complex excavation process of a double-arch tunnel, the rock surrounding the tunnel section changes dynamically during the construction process. Elucidating the state of stress of the surrounding rock during each construction stage at the macroscopic level is crucial for guiding the site operation. Therefore, stress monitoring points are set at the key positions in the left and right lines of the tunnel, such as the arch crown, sidewall, and tunnel bottom, and at the top and bottom of the middle wall. The stress change curve of the double-side-drift method with a temporary vertical support obtained through a calculation is shown in Fig. 4, in which the stress value corresponding to construction stage 0 is the initial stress.

Figures 4 shows that, after the excavation of drifts No. 2 and 4, the stress of the surrounding rock at the arch crown is clearly released. The vertical stress of the surrounding rock of the left arch decreases from 0.11 to 0.04 MPa, and that of the right arch decreases from 0.13 to 0.06 MPa. The vertical stress at the bottom of the left tunnel decreases from 0.3 to 0.02 MPa after the excavation of drift No. 8, and the vertical stress at the bottom of the right line decreases from 0.3 to 0.03 MPa after the excavation of drift No. 11. Large fluctuations in vertical stress on the left and right sidewalls appeared during stages 8 and 14, respectively. The above areas with obvious changes in stress should be considered during the corresponding construction process.

In addition, the vertical stress at the base of the middle partition wall increased steadily from 0.03 to 0.62 MPa after the stress was released owing to the excavation of drift No. 0, indicating that the middle wall starts to act as a load-bearing member after lapping with the steel arches of drifts No. 3 and 4. Therefore, the monitoring and measurement of the middle wall should be strengthened after the middle wall starts to play a load-bearing role.

4.2 Displacement characteristics of the surrounding rock

An analysis of the displacement field in the surrounding rock is important during the construction of a double-arch tunnel. The displacement of the surrounding rock can directly reflect the relative merits of the construction methods. Figure 5 shows the displacement contours of the surrounding rock of the three construction methods after completion of the construction. A comparison of the displacement of the arch crown in the left line when applying the three construction methods is shown in Fig. 6. The deformation area caused by the CRD method is clearly larger than that caused by the double-side-drift method. Meanwhile, compared with the CRD method, the double-side-drift method is more favorable for controlling the deformation of the surrounding rock above the middle partition wall. The CRD method resulted in a settlement of 25 mm, approximately twice that of the double-side-drift

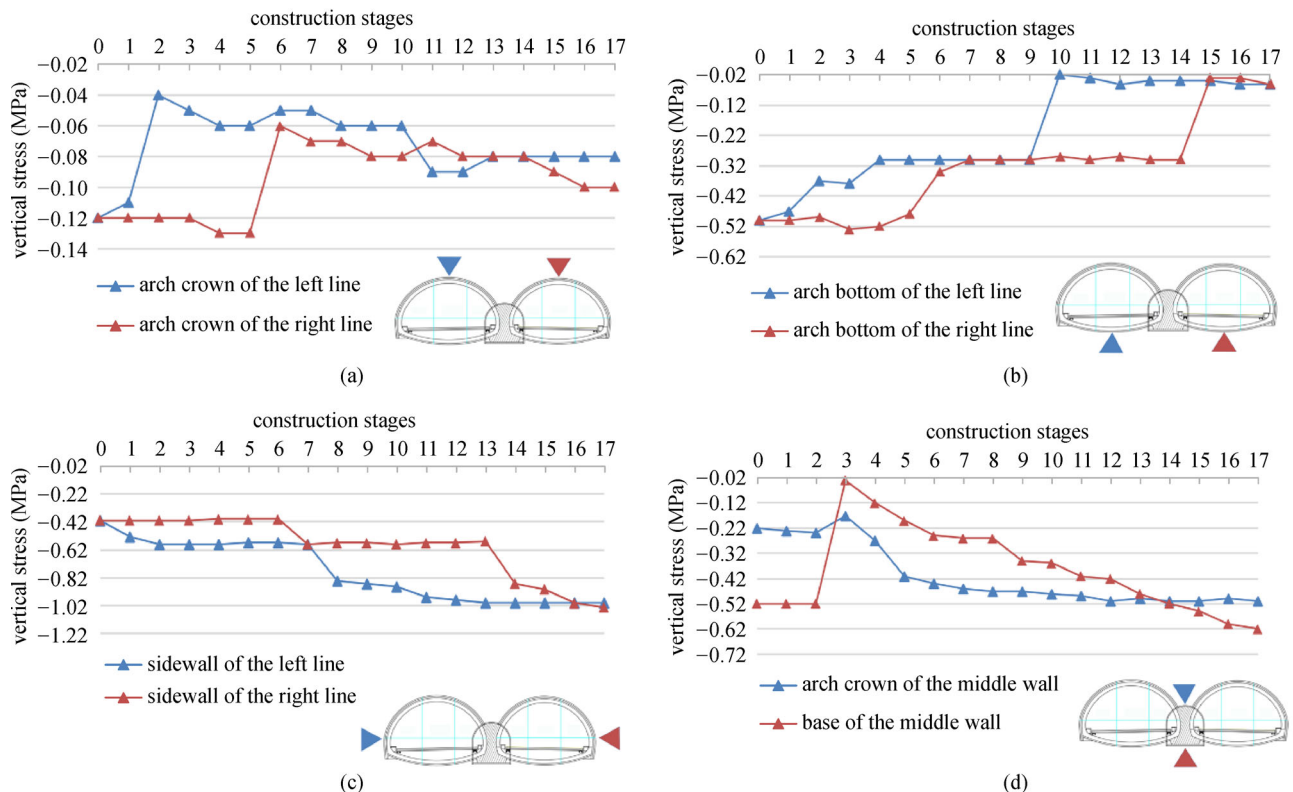


Fig. 4 The vertical stress change curve of the surrounding rock: (a) arch crown; (b) arch bottom; (c) sidewalls; (d) middle wall.

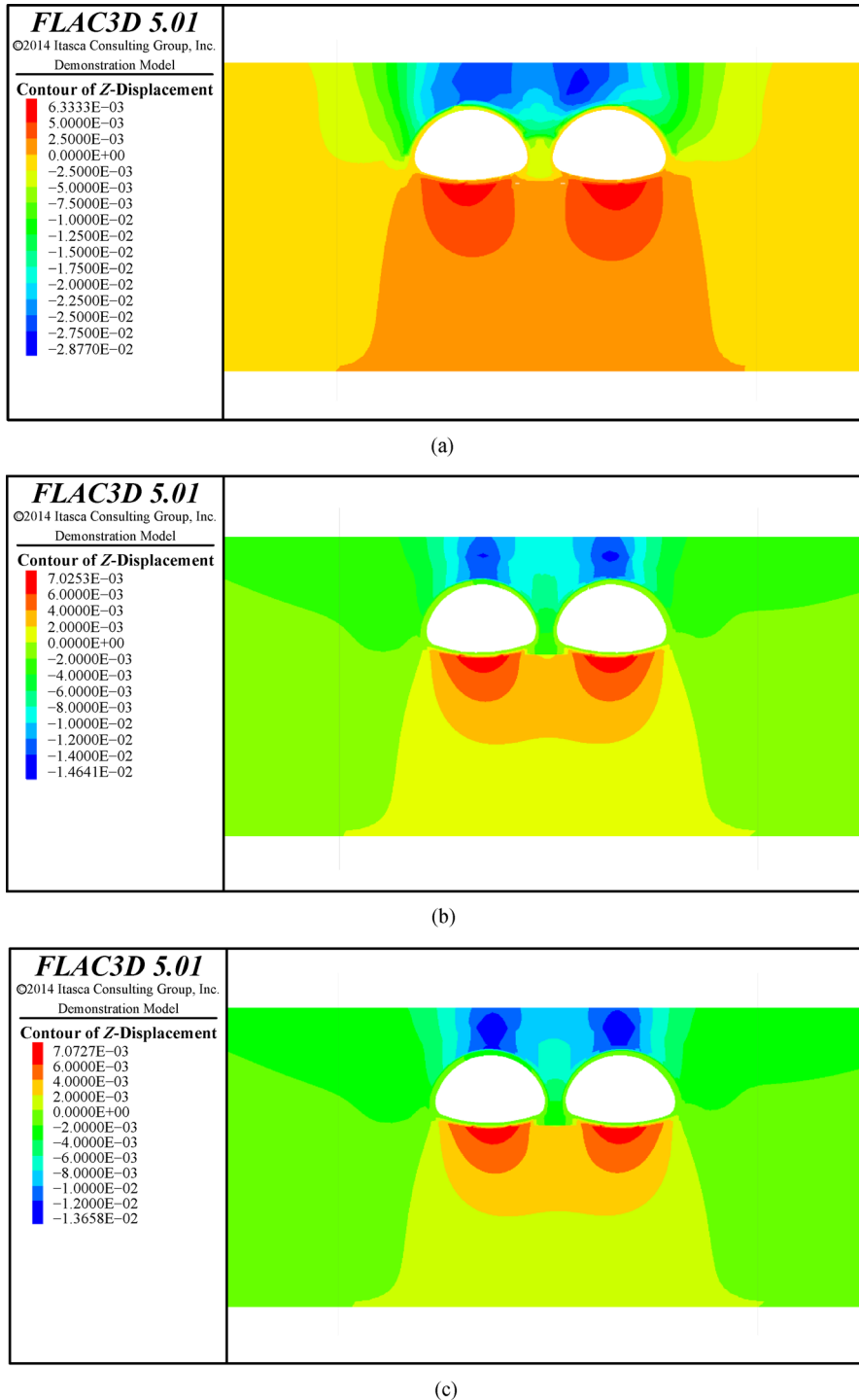


Fig. 5 Comparison of displacement field of surrounding rock: (a) CRD method; (b) double-side-drift method with vertical temporary support; (c) double-side-drift method with curved temporary support (unit: m).

method. A similar settlement of the arch crown can be seen from two types of temporary support forms of the double-side-drift method. The double-side-drift method with a temporary vertical support has slightly better control over the settlement of the arch crown than this method with a temporary curved support.

The displacement contours during each stage of the double-side-drift method with a temporary vertical support are shown in Fig. 7. The surrounding rock deformation caused by the excavation of each drift is similar to the displacement distribution caused by the excavation of a single-arch tunnel. The surrounding rock deformation is

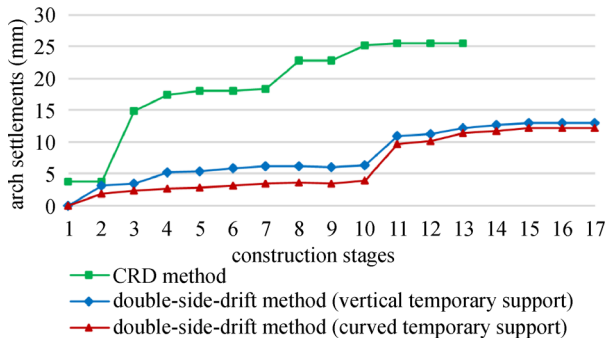


Fig. 6 Comparison of arch crown settlement of three construction methods.

mainly a vertical displacement, which appears in the arch area of each drift and changes dynamically. After completion of the tunnel construction, the maximum vertical displacement of the surrounding rock is approximately 13 mm at the arch crown in the left and right tunnels, and the amount of uplift at the arch bottom is approximately 7 mm. The deformation zone of the surrounding rock extends to the surface, resulting in a maximum surface settlement of approximately 12 mm. The main reason for this result is the shallow burial depth of the tunnel. The maximum horizontal displacement is approximately 6 mm, which occurs at the surface above drifts No. 1 and 6.

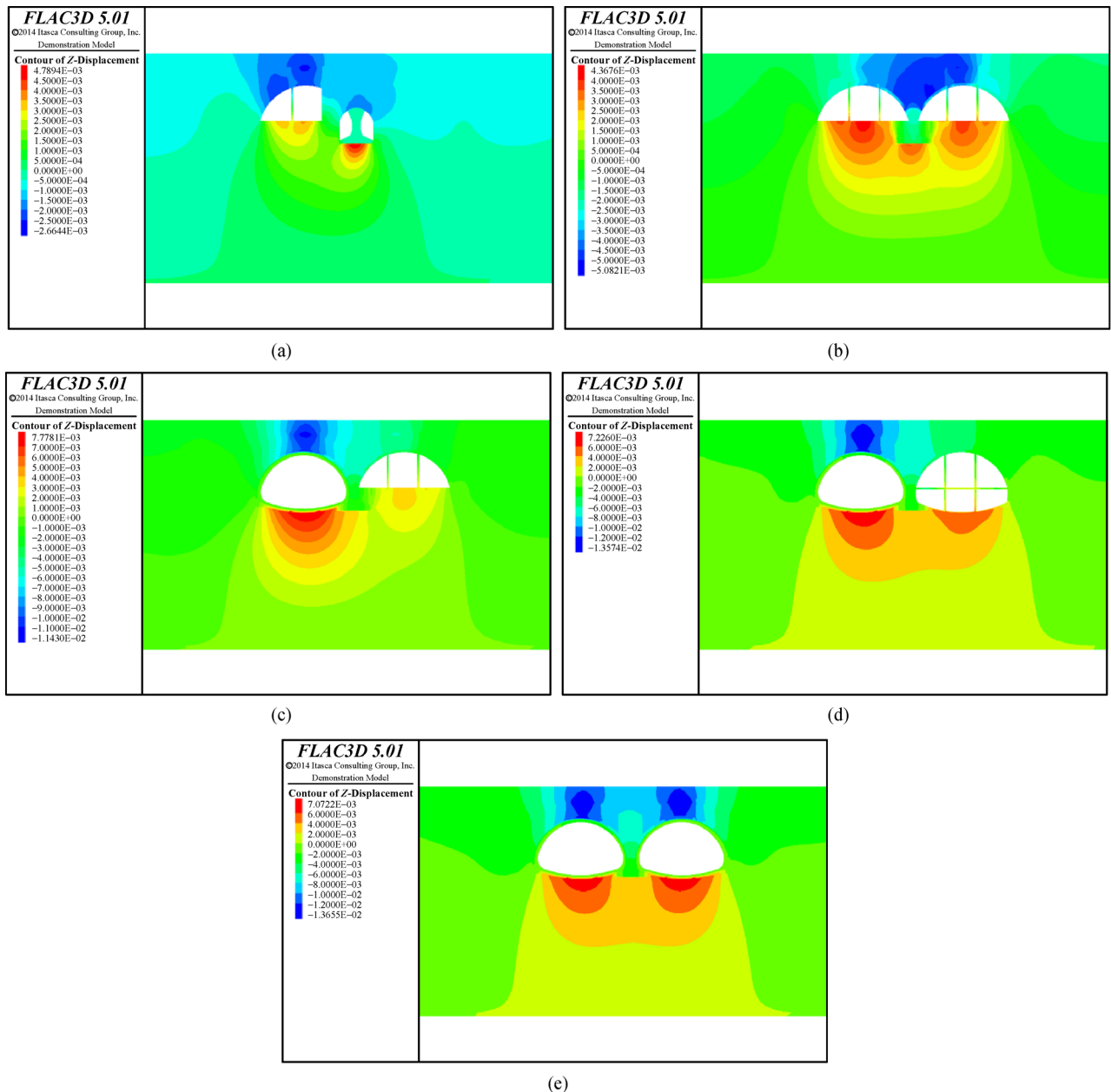


Fig. 7 Displacement contours of the surrounding rock of double-side-drift method with vertical temporary support (unit: m).

In addition, the settlement of the arch crown is an important metric of the construction safety and stability of the surrounding rock. The calculated arch settlements of drifts No. 1–6 change during the construction when applying the double-side-drift method with a temporary vertical support, as shown in Fig. 8.

As shown in Fig. 8, the excavation of drift No. 0 produces a disturbance in the surrounding rocks on both sides of the middle wall, and the deformation in the surrounding rocks accounts for approximately 15% of the final deformation. In addition, the changes in the arch settlement in drifts No. 1, 3, 4, and 6 are similar, and large changes in the displacement curves of drifts No. 2 and 5 occur after the completion of stages 11 and 16. These fluctuations indicate that the removal of the temporary support has a significant impact on the stability of drifts No. 2 and 5. After the removal of the temporary support, an approximately 5 mm arch settlement occurs in the double-arch tunnel, accounting for approximately 45% of the final deformation. Thus, the tertiary lining should be closed as soon as possible after the temporary support is removed to limit further deformation of the surrounding rock.

5 Site monitoring

Finally, the optimized double-side-drift method was adopted in field construction. As shown in Fig. 9, the *in situ* monitoring data of arch settlement of the three drifts are compared with the numerical results. The construction process of the numerical simulation is more ideal than that of the field construction. Therefore, the values of the *in situ* monitoring data are slightly larger than those of the numerical results. However, the variation trend of the *in situ* monitoring data are consistent with the numerical results.

As shown in Figs. 9(a) and 9(b), after completion of stage 10 (the removal of the temporary support), the arch settlement of drifts No. 1 and 3 underwent significant

changes. The same change occurred after stage 15 in drift No. 5. After the removal of the temporary support, an arch settlement of approximately 4.5 mm occurs, generating approximately 40% of the final deformation. The removal of the temporary vertical support has a significant impact on the stability of the double-arch tunnel, as revealed through both numerical simulation and *in situ* monitoring data.

6 Discussion

During the actual tunnel construction, the excavation section of drift using the CRD method is much larger than that using the double-side-drift method. Therefore, it takes longer for the CRD method to complete the excavation and support of a single drift than that of the double-side-drift method. Moreover, the construction difficulty of the temporary vertical support is easier to control than that of the temporary curved support. Therefore, the advantage of the double-side-drift method is more obvious during the actual construction than in the numerical results.

During the construction of the double-arch tunnel, the disturbance of the surrounding rock using the double-side-drift method is frequent, which leads to complicated changes in the stress and displacement fields of the surrounding rock. During the excavation of the drifts, the influence of the excavation of the adjacent drifts is extremely obvious. The deformation area of the surrounding rock changes dynamically with continuous construction. Vertical deformations are mainly concentrated in the arch crown and tunnel bottom. Moreover, because the burial depth of the double-arch tunnel is only 6.8 m, the surrounding rock deformation area extends to the surface, resulting in a surface settlement of approximately 12 mm.

In particular, the application of a triple-layer composite liner system in a large-span tunnel, particularly in a double-arch tunnel with an extra-large span, deserves a more in-depth study. In the future, the authors will focus on a

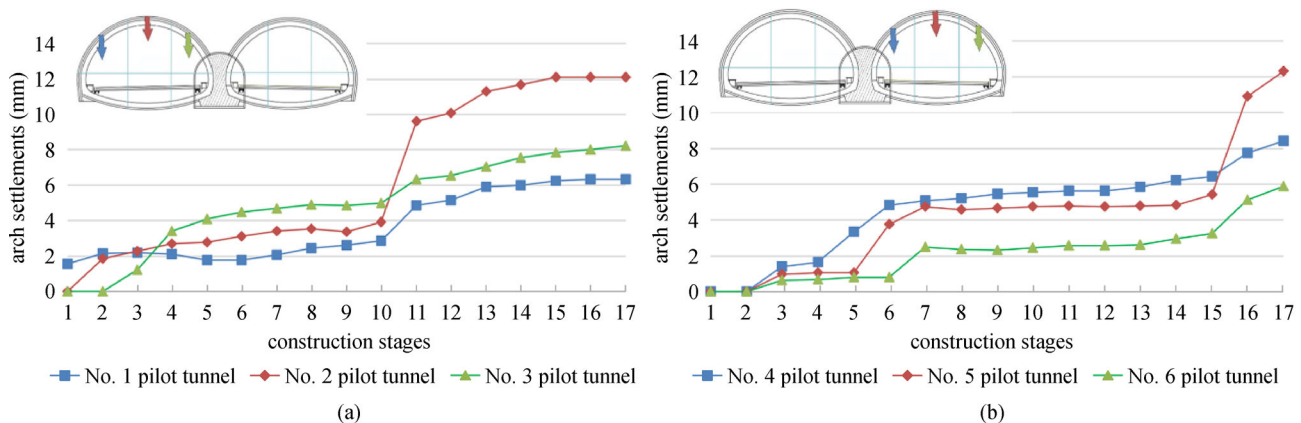


Fig. 8 The relation curves of arch crown settlement and excavation stages of tunnel: (a) left line; (b) right line.

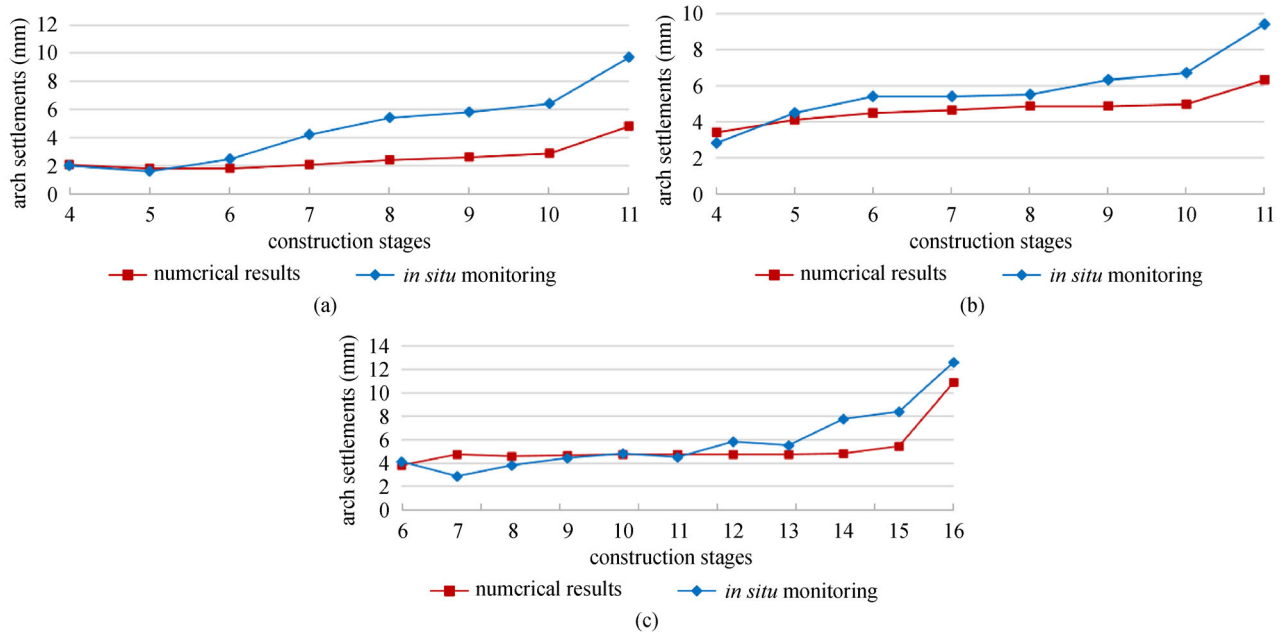


Fig. 9 Comparison of numerical results and *in situ* monitoring data: (a) No. 1 drift; (b) No. 3 drift; (c) No. 5 drift.

theoretical derivation and analysis of the support impact of the flexibility of the primary and secondary supports. In addition, different layouts of the two layers of steel arch frames and other aspects need to be considered.

7 Conclusions

1) During the construction process of the extra-large double-arch tunnel, the excavation section of the drifts when using the double-side-drift method is small and the support is timely. The ability to control the bearing capacity and deformation when using the double-side-drift method is far better than that of the CRD method. The support of the double-side-drift method with a temporary vertical support is slightly better than that with a temporary curved support, and can better meet the requirements of construction space.

2) A temporary vertical support plays a key role in controlling the surrounding rock deformation. The removal of such a temporary support causes varying degrees of impact on the surrounding rocks of each drift. The settlement of the arch crown caused by the removal of the temporary support when applying the double-side-drift method generated approximately 45% of the final settlement.

3) When adopting the double-side-drift method, the compressive stress of the surrounding rock at the sidewall was shown to be less than that of the CRD method. The tensile stress area was the largest when the CRD method was adopted, and the tensile stress area was the smallest when the double-side-drift method with a temporary

vertical support was adopted. The double-side-drift method with a temporary vertical support is more beneficial to the stress redistribution of the surrounding rock in the construction of a double-arch tunnel with an extra-large span.

Acknowledgements Much of the research presented in this paper was supported by the National Natural Science Foundations of China (Grant Nos. 51379112, 51422904, 40902084, 41772298, and 41877239), the Fundamental Research Funds for the Central Universities (No. 2018JC044), and the Shandong Provincial Natural Science Foundation (No. JQ201513).

References

- Li S, Yuan C, Feng X, Li S. Mechanical behaviour of a large-span double-arch tunnel. *KSCE Journal of Civil Engineering*, 2016, 20(7): 2737–2745
- Wang S, Li C, Wang Y, Zou Z. Evolution characteristics analysis of pressure-arch in a double-arch tunnel. *Tehnicki Vjesnik-Technical Gazette*, 2016, 23: 181–189
- Li P, Zhao Y, Zhou X. Displacement characteristics of high-speed railway tunnel construction in loess ground by using multi-step excavation method. *Tunnelling and Underground Space Technology*, 2016, 51: 41–55
- Zhou S, Zhuang X, Rabczuk T. Phase-field modeling of fluid-driven dynamic cracking in porous media. *Computer Methods in Applied Mechanics and Engineering*, 2019, 350: 169–198
- Li P, Zhao Y. Performance of a multi-face tunnel excavated in loess ground based on field monitoring and numerical modeling. *Arabian Journal of Geosciences*, 2016, 9(14): 640
- Zhou S, Zhuang X, Rabczuk T. Phase field modeling of brittle compressive-shear fractures in rock-like materials: A new driving

- force and a hybrid formulation. *Computer Methods in Applied Mechanics and Engineering*, 2019, 355: 729–752
7. Sharifzadeh M, Kolivand F, Ghorbani M, Yasrobi S. Design of sequential excavation method for large span urban tunnels in soft ground–Niayesh tunnel. *Tunnelling and Underground Space Technology*, 2013, 35: 178–188
 8. Zhou S, Rabczuk T, Zhuang X. Phase field modeling of quasi-static and dynamic crack propagation: COMSOL implementation and case studies. *Advances in Engineering Software*, 2018, 122: 31–49
 9. Zhou S, Zhuang X, Rabczuk T. A phase-field modeling approach of fracture propagation in poroelastic media. *Engineering Geology*, 2018, 240: 189–203
 10. Zhou S, Zhuang X, Zhu H, Rabczuk T. Phase field modelling of crack propagation, branching and coalescence in rocks. *Theoretical and Applied Fracture Mechanics*, 2018, 96: 174–192
 11. Zhao X, Chen H, Wang C. Resistance of large deformation of the Wushaoling Tunnel F7 soft fault. *Frontiers of Architecture and Civil Engineering in China*, 2007, 1(1): 123–127
 12. Gao F, Xue D. Double-arch tunnel construction in large span bias weak surrounding rock. *Journal of Chongqing Jiaotong University (Natural Science)*, 2014, 33: 30–34
 13. Yang J, Gou D, Zhang Y. Field measurements and numerical analyses of double-layer pipe roof reinforcement in a shallow multiarch tunnel. *Transportation Research Record: Journal of the Transportation Research Board*, 2008, 2050(1): 145–153
 14. Bai J, Zhao S, Qi B, Yang K. Study on the structure deformation of large-span shallow-buried multi-arch tunnel in soft stratum. *China Civil Engineering Journal*, 2017, 50: 45–50
 15. Yang K, Dong F, Zhang Y, Zhang Z, Huang J. Study on the key technology of urban large span double arch tunnel using drilling and blasting method. *Technology of Highway and Transport*, 2018, 34: 24–32 (in Chinese)
 16. Zhang Y, Shi Y, Zhao Y, Fu L, Yang J. Determining the cause of damages in a multiarch tunnel structure through field investigation and numerical analysis. *Journal of Performance of Constructed Facilities*, 2017, 31(3): 04016104
 17. Wei J, Sun S. Ground Settlement Model for Excavation of a Non-Partial Pressure and Shallow Buried Double-Arch Tunnel. Berlin, Heidelberg: Springer, 2008
 18. Shen Y, Zhao Y, Zhang H, Guo W, Lin Z, Wan Y, Zhang H, Li Z. Numerical analysis of elastoplastic finite element in construction of twin-arch tunnel. *Chinese Journal of Rock Mechanics and Engineering*, 2004, S2: 4946–4951 (in Chinese)
 19. Wang J, Xia C, Zhu H, Li Y, Lin Z, Chen X. Site monitoring and analysis of non-symmetrical multi-arch highway tunnel. *Chinese Journal of Rock Mechanics and Engineering*, 2004, 2: 267–271 (in Chinese)
 20. Ji M, Wu S, Gao Y, Ge L, Li X. Construction monitoring and numerical simulation of multi-arch tunnel. *Rock and Soil Mechanics*, 2011, 32: 3787–3795 (in Chinese)
 21. Dong J. Xiamen second west passage project. *Tunnel Construction*, 2019, 39(5): 890–897 (in Chinese)
 22. Karakus M, Fowell R. Effects of different tunnel face advance excavation on the settlement by FEM. *Tunnelling and Underground Space Technology*, 2003, 18(5): 513–523
 23. Wang Y, Xin Y, Xie Y, Li J, Wang Z. Investigation of mechanical performance of prestressed steel arch in tunnel. *Frontiers of Structural and Civil Engineering*, 2017, 11(3): 360–367
 24. Kong F, Shang J. A validation study for the estimation of uniaxial compressive strength based on index tests. *Rock Mechanics and Rock Engineering*, 2018, 51(7): 2289–2297